



## Experimental investigations of Per- and Poly-fluoroalkyl substances (PFAS) degradation by non-thermal plasma in aqueous solutions

David Alam<sup>a</sup>, Samiuela Lee<sup>a</sup>, Jungmi Hong<sup>a</sup>, David F. Fletcher<sup>a</sup>, Dale McClure<sup>a,b</sup>, David Cook<sup>c</sup>, PJ Cullen<sup>a</sup>, John M. Kavanagh<sup>a,\*</sup>

<sup>a</sup> School of Chemical and Biomolecular Engineering, The University of Sydney, 2006, Australia

<sup>b</sup> Department of Chemical Engineering, College of Engineering, Design and Physical Sciences, Brunel University, Uxbridge, London UB8 3PH, UK

<sup>c</sup> Ventia Australia Pty Ltd, North Sydney, NSW, 2060, Australia

### ARTICLE INFO

Editor: Xin Yang

#### Keywords:

Non-thermal plasma  
PFAS destruction  
Advanced Oxidation Process  
Persistent pollutants  
Per- and Poly-fluoroalkyl Substances

### ABSTRACT

The treatability of perfluorocarboxylic acids (PFCA) (perfluorobutanoic acid (PFBA), perfluorohexanoic acid (PFHxA), perfluorooctanoic acid (PFOA) and perfluorodecanoic acid (PFDA)) and perfluorosulfonic acids (PFSA) (PFBS, Perfluorooctanesulfonic acid PFHxS and Perfluorooctanesulfonic acid (PFOS)) via a bubble column with non-thermal plasma discharges in the argon headspace were investigated in individual solutions and from surface water sourced from a contaminated site. High degradation (>90%) could be achieved for PFOA, PFHxS and PFOS within 40 min treating the contaminated surface water. Overall, treatability correlated with the length of the perfluorinated carbon chain, with a decrease in treatability associated with a reduction of the length of the perfluorinated backbone. Experiments with prepared PFAS solutions at initial concentrations of 10, 25 and 50 µg/L found higher initial concentrations of PFCA and PFSA were associated with faster degradation rates suggesting the treatment efficiency was limited by mass transfer of PFAS. Negligible breakdown was observed for PFBA at any of the concentrations trialled, indicating limitations when treating more hydrophilic PFAS, which may require combining this treatment approach with a polishing step, such as nanofiltration.

### 1. Introduction

The term Per- and Poly- fluoroalkyl Substances (PFAS) encompasses over 5000 compounds containing either completely fluorinated (perfluorinated alkyl substances) or partially fluorinated (polyfluorinated alkyl substances) hydrophobic alkyl chains [1]. Of particular concern are the perfluoroalkyl acids (PFAA) with the general chemical formula  $C_nF_{2n+1}X$ , whereby X represents a charged functional moiety (e.g. carboxylic (-COOH), sulfonic (-SO<sub>2</sub>OH) or phosphonic (-PO(OH)<sub>2</sub>) acids). [2,3]. Due to the high stability of the carbon-fluorine bond, many PFAS are chemically and thermally stable and, depending on the structure, can act as surfactants with exceptional hydrophobic and lipophobic properties [4]. These compounds historically found usage in industrial applications involving severe conditions, such as chrome electroplating of metal [5] and in consumer applications in stain-resistant textile and paper coating formulations [4,6,7]. Compounds such as perfluorooctanoic acid (PFOA) and perfluorosulfonic acid (PFOS) were widely used in these applications until their phase-out and formal

classification as persistent organic pollutants (POPs) after they were found ubiquitously present in the environment, even in remote Arctic regions [8–10].

The use of Aqueous Film Forming Foam (AFFFs), which historically contained PFAS, has also contributed to extensive environmental pollution as these were commonly used to extinguish hydrocarbon-fuel fires at military bases, airports and firefighting training facilities worldwide [11]. These foams float on the top of flammable liquids to extinguish flames by forming a barrier to prevent oxygen contact with the liquid, allowing vapours to escape and to cool surfaces to prevent re-ignition [4]. After use, these foams were generally washed away into drainage systems which allowed these pollutants to enter into surface waters or permeate through the soil into groundwater aquifers, allowing contamination to spread several kilometres from the initial usage site [12–14]. Additionally, these PFAS can enter the environment due to the shedding of material during typical usage, washing and during their disposal, as the anaerobic biodegradation of PFAS coated textiles and carpets in landfill can liberate the PFAS molecules, allowing them to

\* Corresponding author.

E-mail address: [john.kavanagh@sydney.edu.au](mailto:john.kavanagh@sydney.edu.au) (J.M. Kavanagh).

<https://doi.org/10.1016/j.jece.2023.111588>

Received 10 August 2023; Received in revised form 17 October 2023; Accepted 24 November 2023

Available online 29 November 2023

2213-3437/© 2023 The Author(s). Published by Elsevier Ltd. This is an open access article under the CC BY license (<http://creativecommons.org/licenses/by/4.0/>).

travel through percolated rainwater and contaminate the surrounding areas if this landfill leachate is not properly contained [15]. Studies of communities exposed to PFAS contaminated water found probable links with adverse health effects, including kidney and testicular cancer, elevated cholesterol, pregnancy-induced hypertension, thyroid problems, hormone irregularities, and ulcerative colitis. [16–18].

The remediation of PFAS contaminated water has primarily focused on removing the PFAS by filtration and adsorbent-based processes, including ion-exchange resins [19,20], membrane filtration [21–23] or various activated carbon-based adsorbents [24–26]. These processes have shown applicability for removing PFAS from water; however, these processes produce a concentrated PFAS-laden waste stream or spent adsorbent material, which presents additional logistical issues to transport and disposal via an environmentally safe method.

To avoid these issues, technologies capable of destroying PFAS directly in contaminated waters has led to treatment strategies, including sonochemical [27,28] and hydrothermal alkaline treatment (HALT) [29–31] which can directly destroy PFAS in contaminated waters but suffer from low energy efficiency or require the addition of caustic chemicals and high temperatures. More advanced remediation methods utilising electrochemical oxidation/reduction [32–34] and non-thermal plasma [35,36] directly interfaced with contaminated water have shown potential for more energy-efficient destruction of PFAS under ambient conditions. These treatment processes can be done directly on-site to avoid the risks and additional expenses of transporting PFAS-contaminated material to waste treatment facilities. These processes expose PFAS to highly active radical species ( $\text{OH}^-$ ,  $\text{O}_2^-$ ,  $\text{O}$ ,  $\text{H}$ ) and solvated electrons ( $e_{\text{aq}}^-$ ), which can mineralise PFAS via reductive pathways [37–40]. Each of these treatment methods utilises electricity to generate radical species; however, the lower power densities used by electrochemical oxidation requires much longer treatment times of up to 10 h to achieve high levels of breakdown [41,42].

Non-thermal plasma based PFAS destruction processes can interface a plasma directly with the PFAS-contaminated water, interfacing the PFAS with the highly active radical species and effectively mineralising them. Different plasma reactor designs have been trialled for the degradation of PFAS, including Reverse Vortex Gliding Arc [43], falling film reactors [35], and preconcentration by bubbling with surface discharge [36,44], with this latter approach exhibiting greater potential for scalability, and has been trialled at working treatment volumes of 300 L, whereas the other treatment strategies were trialled at a 1 L scale [45]. This treatment approach exploits the strong surfactant nature of PFAS which accumulate at the gas-liquid interface of the bubble which

rises to the surface, enriching the localised concentration of PFAS by several orders of magnitude [46]. The plasma discharge then directly exposes the PFAS at the liquid surface to introduce short lived radical species and solvated electrons into the water, as well as bombarding the surface with highly energetic ionised gaseous species which can further facilitate breakdown [47]. Additionally, with sufficient energy input, the plasma channel can reach sufficiently high temperatures ( $>2000$  K), to achieve thermal decomposition of PFAS [48]. The experimental studies aim to investigate further and improve the understanding of the applicability and treatability of PFAA via plasma treatment by investigating their respective degradation rates in prepared PFAS solutions and real-world contaminated surface water samples.

## 2. Materials and methods

### 2.1. Experimental setup

The treatment reactor shown in Fig. 1 consisted of a 200 mm tall, 150 mm OD (140 mm ID) acrylic tube with 50 mm wide flanges on both ends which could be sealed with an acrylic plate. The total volume inside the reactor was  $\approx 3.1$  L, with a working volume of 2 L of liquid used for all experiments. A carborundum dome-shaped diffuser (60 mm OD, 30 mm tall) was positioned in the centre on the base of the reactor and connected with flexible tubing to an Alicat (USA) mass flow controller (MCS-10SLPM-D) supplying argon at 1 L/min. Argon gas was used as the plasma working gas as it has a low breakdown voltage of 2.7 kV/cm compared with air at 32 kV/cm, allowing for the gas to be easily ionised into plasma while also being more available and economical compared with helium or other noble gases [49].

At this flow rate, the diffuser produced bubbles ranging in diameter from 2 to 5 mm, with a Sauter mean diameter of 3.8 mm based on the frequency distributions from characterising a series of images that contained a total of 1200 bubbles. The bubble sizing methodology determined the bubble size, assuming an equivalent diameter for a circle based on the quantified projected area of the bubbles. Further details of the methodology have been included in the [Supplementary Information](#). A series of 8 tungsten carbide tipped rods were used as the high voltage electrodes and were connected to a power distributor which rotated at a rate of  $\approx 500$  rpm cycling the plasma discharge through each electrode several times per second to allow for a larger overall liquid surface area to be interfaced with plasma. The ground electrode consisted of a 6.35 mm stainless steel rod inserted through the lid directly into the liquid and connected to the return wire of the power supply.

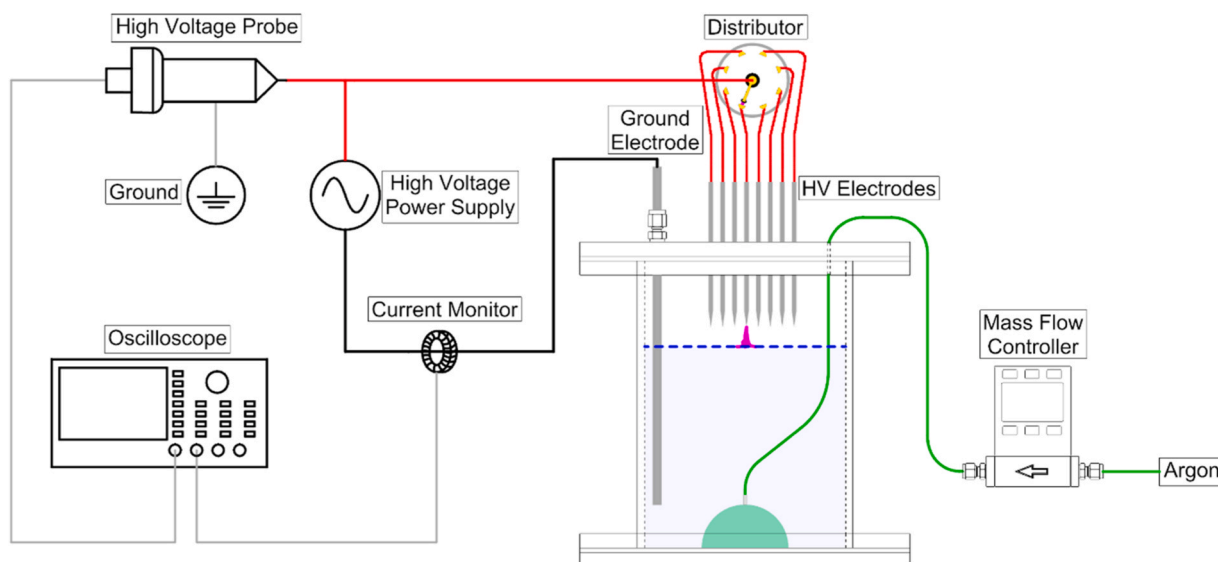


Fig. 1. Schematic diagram of the plasma treatment reactor.

A Plasmaleap (Australia) Leap100 high-voltage, high frequency micropulse generator was used to produce the plasma discharges. A peak-to-peak voltage of  $3.5 \pm 0.3$  kV oscillating at 58.00 kHz and pulse frequency of 1000 Hz was used. A Rigol (China) 4-channel digital oscilloscope (DS6104) was used with a North Star High Voltage (USA) high voltage probe (PVM-6) and Pearson Electronics (USA) current monitor (Model 2877) to measure the voltages and current applied to the discharge electrodes during discharge. The power consumed by the plasma discharge was calculated to be  $4.0 \pm 0.7$  W by integrating the voltage and current waveforms with respect to time. These values were determined based on averaging the results from pentaplicate measurements and calculations and included the standard deviation as a margin of error. Typical voltage and current waveforms have been included in Fig. 2 to present the waveforms of a pair of electrical pulses (left) and over a single pulse (right) to highlight the oscillating nature of these electrical pulses applied to the high voltage electrode.

The optical emission spectra (OES) of the plasma discharge in the gaseous headspace was captured using an Oxford Instruments (UK) Andor Shamrock 500i spectrometer fitted with a Newton DU920P-OE charge-coupled device (CCD) camera. Solis Spectroscopy software from Oxford Instruments was used for the data acquisition and spectrum processing. A fibre optic cable was inserted through the reactor lid and positioned to capture the light from the plasma discharges into the spectrometer.

Liquid samples were taken  $\approx 30$  mm below the surface using a 50 mL polypropylene syringe and stored in certified PFAS-free HDPE sample bottles for later analysis by liquid chromatography-tandem mass spectrometry (LC-MS/MS) and ion chromatography (IC). The syringe was filled and emptied 5 times before acquiring and transferring the liquid sample into the sample bottle. Samples were taken before treatment and after 5, 10, 15, 20, 40, 60, 90 and 120 min of plasma treatment.

## 2.2. Chemicals

Aqueous stock solutions of each PFAS investigated were prepared to a concentration of  $\approx 50,000$   $\mu\text{g/L}$  in deionised water using the following chemicals sourced from Sigma Aldrich (Australia) without further purification: Perfluorobutanoic acid (PFBA, 98%), Perfluorohexanoic acid (PFHxA, 97%), Perfluorooctanoic acid (PFOA, 95%), Perfluorooctanesulfonic acid (PFOS,  $\approx 40\%$  in  $\text{H}_2\text{O}$ ), Perfluorodecanoic acid (PFDA, 98%) Perfluorohexanesulfonic acid (PFHxS, 98%) and Perfluorobutanesulfonic acid (PFBS, 97%). Before an experiment, 0.5–2 mL of the stock solutions were added into the treatment reactor and mixed into 2 L of an aqueous solution containing  $\approx 2.4$  mM sodium chloride ( $\approx 300 \pm 1$   $\mu\text{S/cm}$ ) prepared with reverse osmosis water to reach the

required PFAS concentration of 10, 25 or 50  $\mu\text{g/L}$ .

## 2.3. Contaminated surface water composition

The contaminated surface water was sourced from a concrete lined, storage pond from an undisclosed site within Australia with a known history of fire-fighting foam usage and was found to contain a total of 15 different PFAS species, including a range of perfluorocarboxylic acids (PFCA), perfluorosulfonic acids (PFSA) and fluorotelomersulfonic acid (FTS) of varying carbon chain length from 4 to 10 as shown in Table 1. A total of 29.7  $\mu\text{g/L}$  of PFAS was detected in the surface water with PFOS accounting for 62% of the total concentration of PFAS present in the surface water at 18.5  $\mu\text{g/L}$ .

Water quality parameters of the contaminated surface water were tested by Envirolab Services (Australia), including cation composition, pH, conductivity, and alkalinity (Supplementary Information, Table S1). The surface water was found to have a conductivity  $\approx 320$   $\mu\text{S/cm}$  and pH of 7.4, indicating it was slightly alkaline owing to the presence of 44 mg/L of bicarbonate ions. Sodium ions were found to be in the greatest abundance at 33 mg/L, followed by calcium at 7.2 mg/L, potassium at 2 mg/L and magnesium at only 1 mg/L. Additionally, a Methylene Blue Active Substances (MBAS) assay was undertaken to detect any anionic surfactants that could have been present due to contamination by other surfactants; however, none could be detected above the detection limits of 0.1 mg/L. [50].

## 2.4. Liquid chromatography-tandem mass spectrometry (LC-MS/MS)

A Thermo Scientific (USA) TSQ Altis triple quadrupole mass spectrometer was used to analyse samples by LC-MS/MS. The elution solvent consisted of a binary solvent mixture of: (A) 98 vol% deionised water, 2 vol% methanol, 0.1 vol% acetic acid and 2 mM ammonium acetate, and (B) 98 vol% methanol, 2 vol% deionised water 0.1 vol% acetic acid and 2 mM ammonium acetate. The methanol used was LC-MS grade, whereas the ammonium acetate and acetic acid were of trace metal grade (99.999%) and used without further purification. The gradient elution method given in Table 2 was used at a total flow rate of 0.3 mL/min. The first 2 min of the method were diverted to waste before switching to the MS/MS to prevent inorganic salts from precipitating and blocking the nebuliser.

An Agilent Zorbax Rapid Resolution High Definition (RRHD) Eclipse Plus column (1.8  $\mu\text{m}$  packing,  $3 \times 50$  mm) was used as an isolator column in conjunction with an Agilent Zorbax RRHD StableBond C18 (1.8  $\mu\text{m}$  packing,  $2.1 \times 100$  mm) analytical column for the separation of the PFAS analytes. Samples were injected directly in the LC-MS/MS without

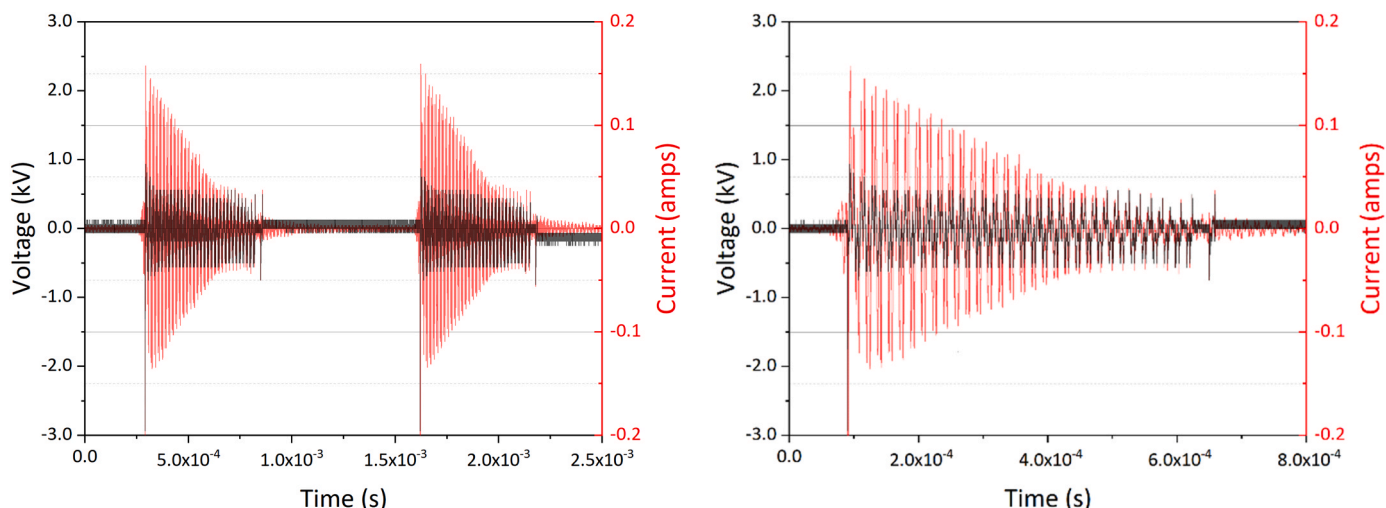


Fig. 2. Voltage and current waveforms over a pair of electrical pulses (left) and a single pulse to more clearly visualise the high frequency oscillations (right).

**Table 1**

Composition of the PFAS contaminated surface water treated categorised based on structure: PFSA (left), PFCA (middle) and FTS (right).

Perfluorosulfonic acid (PFSA)	Conc. ( $\mu\text{g/L}$ )	Perfluorocarboxylic acid (PFCA)	Conc. ( $\mu\text{g/L}$ )	Fluorotelomersulfonic acid (FTS)	Conc. ( $\mu\text{g/L}$ )
Perfluorobutane sulfonic acid (PFBS)	0.26	Perfluorobutanoic acid (PFBA)	0.32	6:2 Fluorotelomer sulfonic acid (6:2 FTS)	2.50
Perfluoropentane sulfonic acid (PFPeS)	0.27	Perfluoropentanoic acid (PFPeA)	0.64	8:2 Fluorotelomer sulfonic acid (8:2 FTS)	0.10
Perfluorohexane sulfonic acid (PFHxS)	3.00	Perfluorohexanoic acid (PFHxA)	3.05		
Perfluoroheptane sulfonic acid (PFHpS)	0.28	Perfluoroheptanoic acid (PFHpA)	0.22		
Perfluorooctane sulfonic acid (PFOS)	18.50	Perfluorooctanoic acid (PFOA)	0.46		
Perfluorodecane sulfonic acid (PFDS)	0.04	Perfluorononanoic acid (PFNA)	0.04		
		Perfluorodecanoic acid (PFDA)	0.03		
<b>Total PFSA</b>	<b>22.35</b>	<b>Total PFCA</b>	<b>4.76</b>	<b>Total FTS</b>	<b>2.60</b>
<b>Total concentration of PFAS detected: 29.7 <math>\mu\text{g/L}</math></b>					

**Table 2**

Gradient elution method used to separate and analyse PFAS analytes.

Time (min)	Composition	
	A	B
0	100	0
2	100	0
3	80	20
8	50	50
15	15	85
16	0	100
19	0	100
19.01	100	0
23	100	0

prior filtration and analysed in triplicate to avoid introducing sampling bias due to analyte retention due to sample filtration [51]. Before analysis, each sample was spiked with a deuterated  $\text{C}^{13}$  mass-labelled PFAS standard mixture (MPFAC-24ES, Wellington Laboratories) containing 19 different isotopically doped PFAS standards used as an internal reference to account for injection recovery.

### 2.5. Ion chromatography

Fluoride ions formed during the defluorination of PFAS were identified using a 930 compact Ion Chromatograph (IC) with ProfIC autosampler and dilution module from Metrohm (Switzerland). A Metrosep A Supp 7 (5  $\mu\text{m}$  packing,  $4 \times 250$  mm) column was used to separate the analytes over 32 min using an isocratic flow rate of 0.7 mL/min of 3.6 mmol/L sodium carbonate. Samples were analysed unfiltered and undiluted with an injection volume of 100  $\mu\text{L}$ . Type I (Ultrapure water) generated by an Elga (UK) PURELAB Quest water purification system was used to prepare the mobile solvent and calibration standards.

## 3. Results and discussion

### 3.1. Plasma treatment of PFAS contaminated surface water

A 2 L volume of the PFAS-contaminated surface water was directly plasma treated for 120 min without prior filtration or dilution. The composition of PFAS in the surface water during plasma treatment markedly changed over time, as shown in Fig. 3. The concentration of PFOS rapidly decreased to half after only 5 min of plasma treatment and reached a  $\approx 99\%$  reduction after 40 min from an initial concentration of 18.5  $\mu\text{g/L}$ . Particularly long chain ( $>6$  carbon) PFSA and FTS showed the highest affinity to degradation by plasma treatment, with a 99.9%, 94.7% and 100% reduction in PFOS, PFHxS and 6:2 FTS after 120 min of treatment which combined accounted for 80.8% of the total PFAS initially detected in the surface water. After 120 min of treatment, long chain PFCA ( $>C8$ ) PFOA, PFNA, and PFDA all reached below detectable levels, while the shorter chain compounds proved more resistant to degradation. Each of the compounds initially detected in the surface water decreased in concentration after plasma treatment, except for PFBA and PFPeA, which accumulated as by-products of the degradation

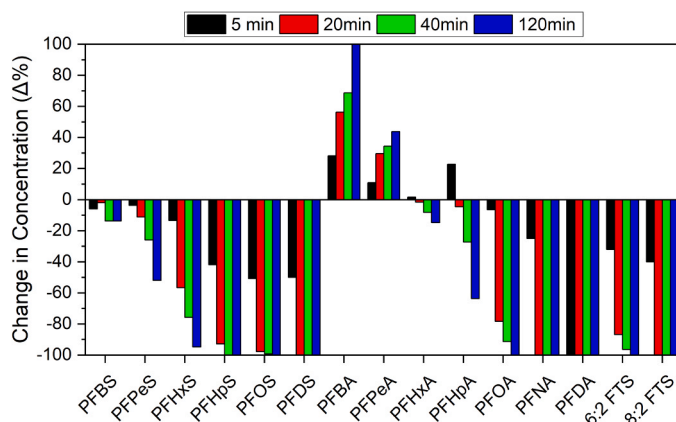


**Fig. 3.** Change in concentration of each PFAS detected in the contaminated surface water compared with the initially detected concentrations after 5, 20, 40 and 120 min of plasma treatment.

of the longer chain analogues. These short chain species steadily rose in concentration over time, increasing by 100% and 43.8% after 120 min of plasma treatment from their initially detected concentrations of 0.32  $\mu\text{g/L}$  and 0.64  $\mu\text{g/L}$ .

As shown in Fig. 3, the breakdown rate of PFAS was at its highest over the first 10 min of plasma treatment with a 63.2% reduction in the total concentration of PFAS, reaching 80.5% after 40 min. Continuing plasma treatment for a further 80 min only resulted in an additional 3.4% reduction in the total concentration of PFAS and reached a maximum of 83.4% breakdown after 120 min. The overall PFAS breakdown rate was found to decrease logarithmically over time as the total PFAS concentration decreased as compounds such as PFOS, PFHxS, and 6:2 FTS reached high levels of degradation, leaving primarily the shorter chain ( $<C6$ ) PFCA compounds in the surface water which were less amenable to degradation (Fig. 4).

Through analysis of the physiochemical properties of these compounds, both the octanol/water partition coefficient ( $K_{ow}$ ) and adsorption coefficient ( $K_i$ ) were found to be reliable indicators of a compound's tendency to degrade during plasma treatment. The  $K_{ow}$  coefficient is defined as the ratio of a chemical's concentration in the octanol phase to its concentration in the aqueous phase in a two-phase octanol/water system, [52], whereas the  $K_i$  coefficient is a measure of the equilibrium concentration of surfactant molecules adsorbed onto the air-water interface, in relation to the concentration of molecules in the bulk liquid solution [53,54]. Each of these coefficients can be used to determine the affinity for a particular compound to adsorb to the gas-liquid interface. The change in concentration after 120 min of plasma treatment of each species and their respective  $K_{ow}$  value is presented in Fig. 5 (Left) and their respective  $K_i$  value in Fig. 5 (Right). The  $K_{ow}$  values were computationally estimated using the EPI Suite™ software package (US EPA) which has been shown to provide reasonable approximations for PFAS, [55,56], whereas the adsorption coefficients were sourced from Brusseau (2019) [57]. Compounds possessing a  $K_{ow}$



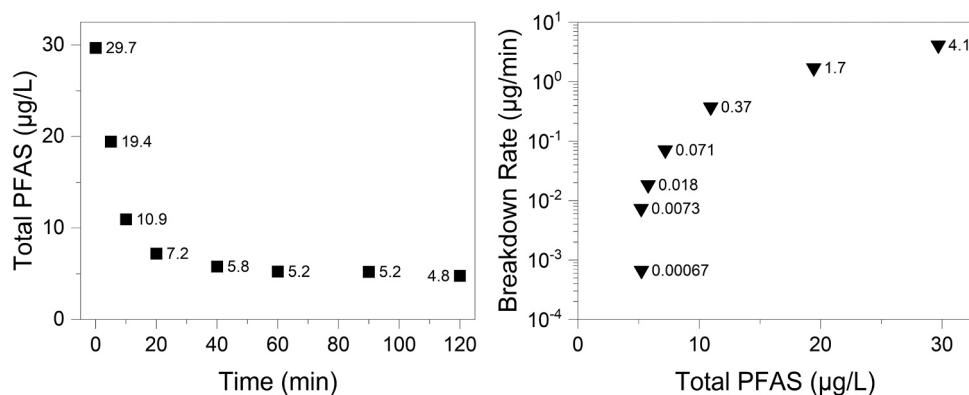


Fig. 4. Total PFAS concentration over time (Left). Breakdown rate against total PFAS concentration (Right).

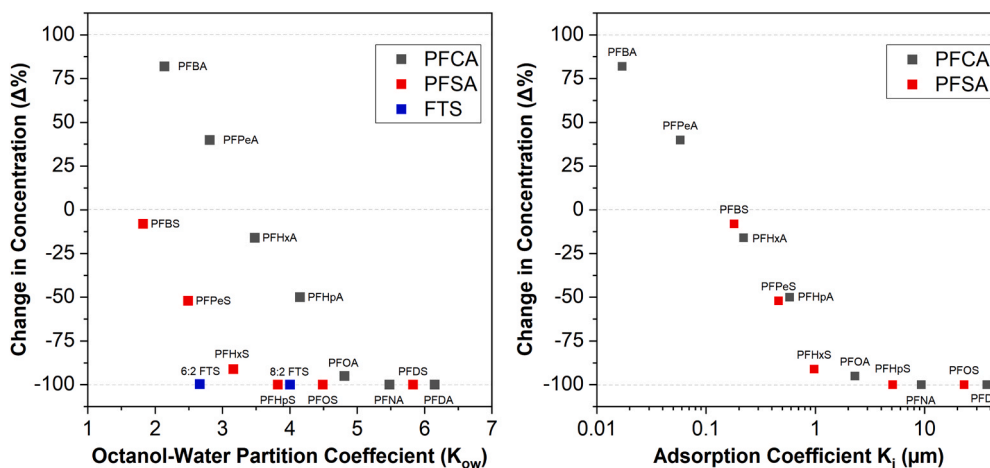


Fig. 5. Relationship between overall change in concentration after 120 min plasma treatment, octanol-water partition coefficients (left), and adsorption coefficients (right) for the PFAS detected in the contaminated surface water treated. Note: adsorption coefficients for the FTS could not be sourced.

value above PFOS (4.49), approached 100% degradation after 120 min of plasma treatment, whereas degradation approached 100% for PFAS with  $K_i$  coefficients  $\geq 1$  µm. These trends are similar to those observed in Murphy et al. (2021) who reported removal of PFAS approached 100% for compounds with adsorption coefficients greater than  $\approx 1$  µm using Surface-Active Foam Fractionation (SAFF) [53]. As the hydrophobicity of the PFAS decreased, they became much less amenable to degradation via this plasma treatment method which relies upon surfactant properties of PFAS to congregate at the air-water interface of the bubble and be transported to the liquid surface for degradation. Of the classes of compounds present in the surface water, FTS were observed to be the most reactive class of PFAS as their structure incorporates two aliphatic carbons, unshielded by fluorine atoms, followed by PFSA and PFCA [58].

### 3.2. Treatment of individual PFAS solutions

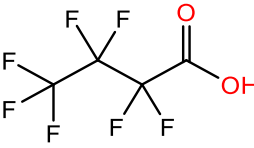
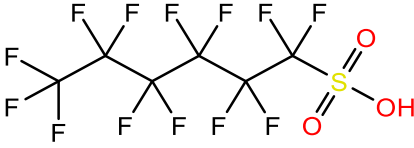
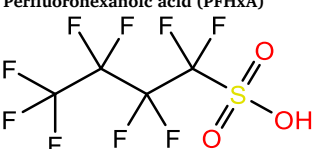
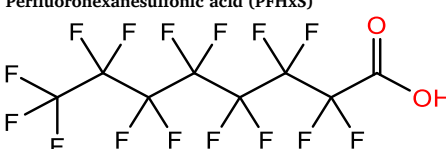
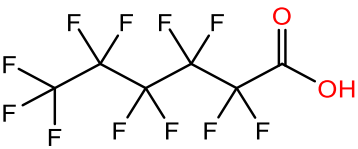
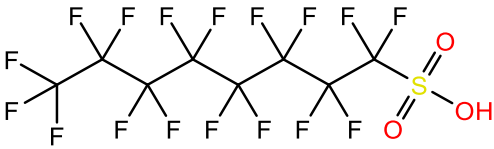
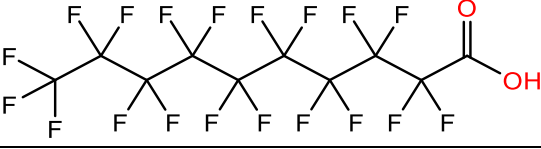
Potential interactions between PFAS during plasma treatment were difficult to discern due to the complicated mixture of compounds. To further the understanding of the PFAS breakdown rates prepared PFAS solutions were treated in the same reactor under the same experimental conditions. The PFCA and PFSA compounds shown in Table 3 with perfluorinated aliphatic carbon lengths varying between 4 and 10 were investigated for treatability for 120 min with an initial concentration of 10, 25 and 50 µg/L in 2 L of  $300 \pm 1$  µS/cm aqueous solution prepared with reverse osmosis water with added sodium chloride to represent background ions.

#### 3.2.1. Degradation of perfluorocarboxylic acids

As shown in Fig. 6, the experimental results demonstrate a strong correlation between chain length and the overall tendency for a compound to breakdown during plasma treatment using the developed reactor. When studying the compounds in their respective individual solutions, it is evident that the decrease in surface activity with a reduction in chain length greatly reduces a compound's degradation rate. This was most clearly observed at an initial concentration of 10 µg/L, with an 87.7%, 61.6%, 21.4% and 0% reduction in PFDA, PFOA, PFHxA and PFBA after 120 min of plasma treatment. At an initial concentration of 50 µg/L and 25 µg/L, PFDA and PFOA showed similar levels of degradation over 120 min plasma treatment due to their hydrophobicity, which were able to accumulate at the gas-liquid interface of the bubbles and subsequently the plasma-liquid interface for destruction. However, at an initial concentration of 10 µg/L, the more strongly hydrophobic PFDA (37 µm) reached a 90% reduction after 120 min of plasma treatment, whereas PFOA (2.3 µm) reached a lower overall degradation of 63%. The breakdown rate of the comparatively less hydrophobic PFOA reduced with decreasing concentrations  $< 5$  µg/L, as fewer molecules could accumulate to rising bubbles and undergo destruction. This decrease in degradation indicates the treatability of a compound is heavily influenced by their structure and relative concentration in the solution, with more strongly hydrophobic compounds able to reach higher overall degradation due to a greater affinity to the gas-liquid interface, further supporting previous observations which saw a logarithmic decrease in breakdown rates as concentration decreased  $< 5$  µg/L.

No quantifiable ( $< 5\%$ ) reduction in the initial concentration of PFBA

**Table 3**  
Structure of the PFCA and PFSA compounds investigated.

Perfluorocarboxylic Acids (PFCA)	Perfluorosulfonic Acids (PFSA)
<b>Perfluorobutanoic acid (PFBA)</b> 	<b>Perfluorobutanesulfonic acid (PFBS)</b> 
<b>Perfluorohexanoic acid (PFHxA)</b> 	<b>Perfluorohexanesulfonic acid (PFHxS)</b> 
<b>Perfluorooctanoic acid (PFOA)</b> 	<b>Perfluorooctanesulfonic acid (PFOS)</b> 
<b>Perfluorodecanoic acid (PFDA)</b> 	

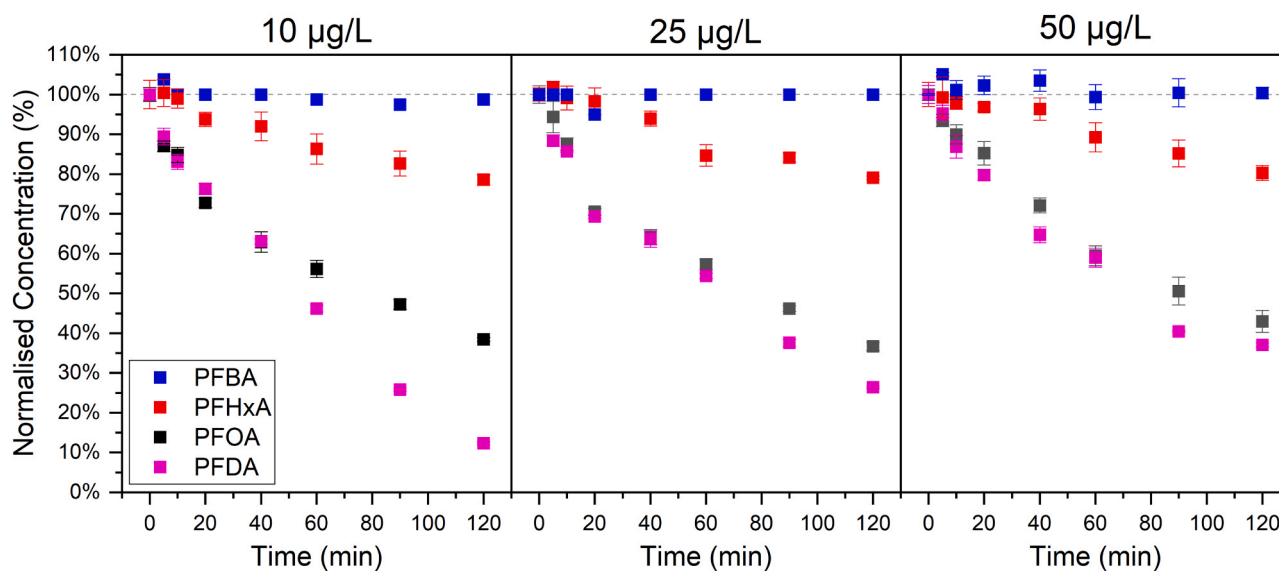


**Fig. 6.** Normalised concentration of each of the PFCAs during plasma treatment at an initial concentration of 10 µg/L (Left), 25 µg/L (Centre) and 50 µg/L (Right).

in the solution could be observed in any of the samples taken over time during plasma treatment, and neither were any breakdown products detected by LC-MS/MS or IC. The concentration of PFBA remained consistent over time for each of the concentrations trialled, indicating that the recovery of this species was effectively 100%. The high recoveries of PFBA detected at each time point were used to conclude that no measurable decomposition had occurred due to plasma treatment,

nor were their significant losses due to aerosol formation or volatilisation due to the mechanical agitation of bubbling or sticking to reactor surface walls.

The addition of cosurfactants as a foaming agent or charged collector has been used in foam floatation experiment studies to aid in removing PFAS from landfill leachate, with cationic surfactants producing the most significant enhancement [59]. Cationic surfactants such as

cetyltrimethylammonium bromide (CTAB) have also been used as a co-surfactant to enhance the destruction of shorter chain PFAS in plasma-based treatment processes, as the positive charge on this surfactant can attract the negative tail of these short chain PFAS to the bubble surfaces and hence transport the molecules to the plasma-liquid interface for destruction [60,61]. However, while destruction of these short chain compounds could be achieved through the use of a cationic surfactant, caution must be exhibited as there is a significant risk of forming unwanted by-products during the plasma treatment such as bromate ( $\text{BrO}_3^-$ ) ions which are difficult to remove by water treatment processes [61]. Investigating alternative cationic co-surfactants or flotation aids to enhance PFAS degradation rate may help to mitigate potential risks in forming these hazardous products and will likely be a key research topic moving forward.

Ideally, a destruction technology would be able to address the full range of short and long chain PFAS simultaneously; however, due to the wide range of chemical properties of PFAS detected in contaminated sites, this will be highly challenging. To more adequately address the remediation of PFAS, a secondary treatment step to remove residual concentrations of PFAS present in plasma-treated streams would be required in a treatment train and could utilise technologies such as nanofiltration or ion-exchange resins to polish the water and meet emission standards [62]. The use of plasma treatment in conjunction with ion exchange resins are particularly advantageous as these adsorbents have been shown to achieve high removal rates for shorter chain PFAS, such as PFBA or PFBS, with polystyrene divinylbenzene (PS-DVB) based resins, [63] but can exhibit competitive adsorption between the

long and short chain PFAS with prolonged contact times (>48 hrs) which displaces the shorter chain PFAS from binding sites on the ion exchange resins and reduces removal efficiency [64]. By initially initial plasma treating the PFAS contaminated water, the long chain, hydrophobic PFAS could be destroyed, allowing the resin to have a higher capacity for removing the shorter-chain species as the competing species that could displace the short chain species from the resin are removed. Furthermore, the use of a plasma-based destruction process as part of a two stage remediation approach would greatly reduce the overall quantities of PFAS in the inlet stream for the polishing step, thereby prolonging the effectiveness of the adsorbent and the time between regeneration cycles or resin bed changes.

The formation of several shorter chain PFCA were detected as the degradation products from each PFCA and concentrations were investigated as shown across the graphs presented in Fig. 7. The total quantity of short-chain products detected by LC-MS/MS was dependent on the initial concentration of the PFCA, the compound's surface activity and breakdown rate. The quantities of shorter-chain PFCA breakdown products represented only a small fraction (<5%) of the total fluorine from the destroyed parent PFCA compound being converted to shorter-chain breakdown products. The proportion of short-chain PFCA detected in these experiments is comparable with findings and recoveries of similar works, which proposed that these short-chain compounds account for  $\leq 10\%$  of the total fluorine in the reactor [65,66]. These results suggest a high degree of mineralisation had occurred due to a combinative approach of thermal decomposition induced by the plasma at the surface and the high energy species contributing as the primary

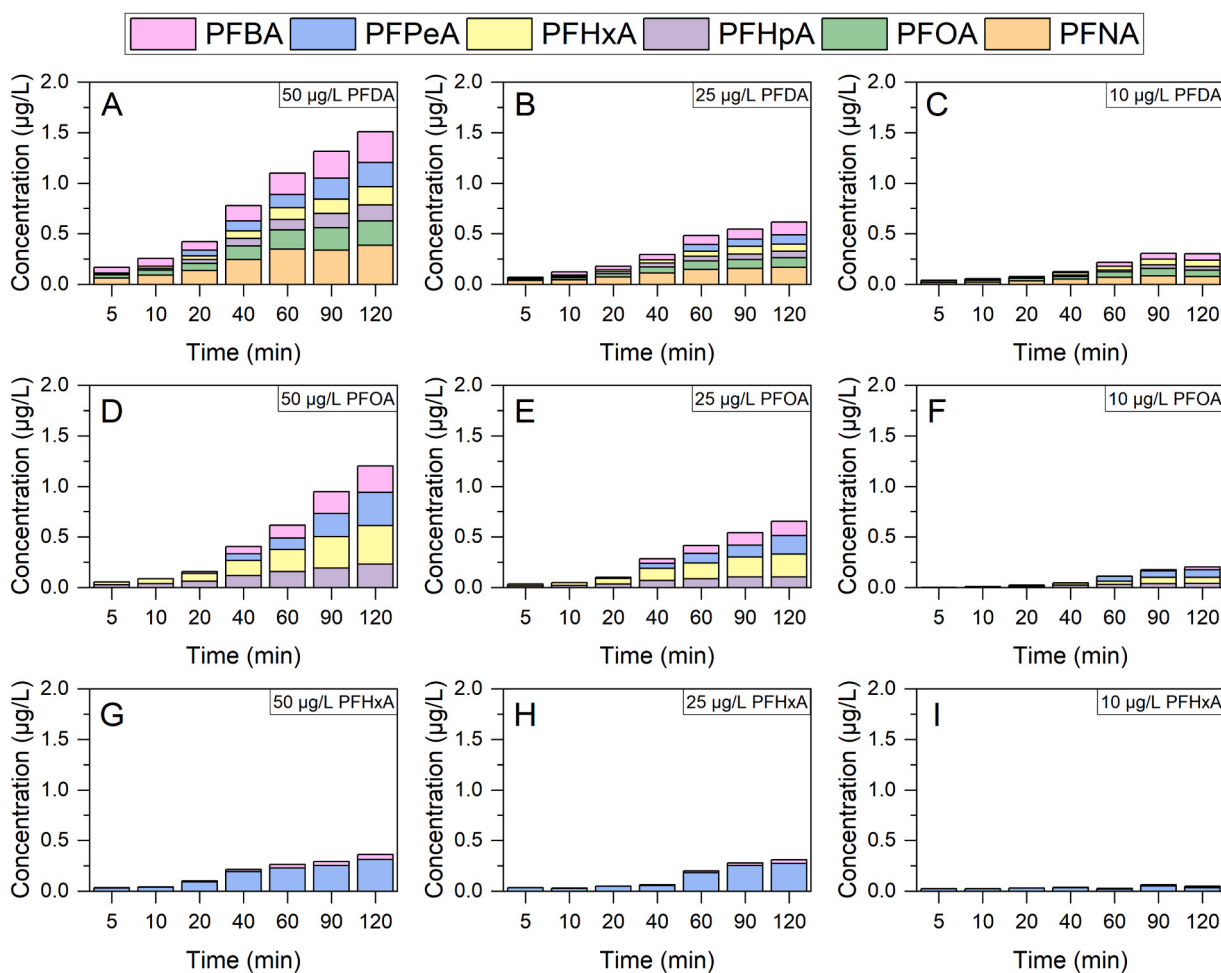


**Fig. 7.** The concentration of the short-chain PFCA detected in the liquid samples over time during plasma treatment. PFDA at 50 µg/L (A), 25 µg/L (B), and 10 µg/L (C), PFOA at 50 µg/L (D), 25 µg/L (E) and 10 µg/L (F), and PFHxA at 50 µg/L (G), 25 µg/L (H), and 10 µg/L (I).

degradation pathways. The formation of gaseous products could not be identified but may have occurred as a result of radical cyclisation reactions of perfluoroalkyl chain radicals, forming cyclic perfluorocarbons containing between 4 and 8 carbons [36].

### 3.3. Degradation of perfluorosulfonic acids

In these experimental investigations, PFBS, PFHxS, and PFOS, were treated under the same experimental conditions, concentrations, and plasma reactor configuration for treatment times up to 120 min to determine the treatability of these PFSA compared with their carboxylic acid analogues. Owing to the similar structures of the compounds investigated, the overall trend in the degradation rate of the PFSA similarly correlated with chain length, as can be seen in the graphs presented in Fig. 8. However, as these compounds possess superior surfactant strength and a greater ability to reduce the surface tension of a liquid compared with their PFCA analogues, [67] the PFSA investigated were found to be more susceptible to degradation as they could be more easily floated to the liquid surface for destruction. In comparison with their carboxylic acid analogues, PFOS reached 86% degradation at 50  $\mu\text{g/L}$  initial concentration compared with PFOA 57% after 120 min of plasma treatment, and unlike PFBA, some decomposition of  $\approx 15\%$  PFBS could be observed at each of the concentrations investigated after the 120 min of plasma treatment as shown in Fig. 8.

The quantified breakdown products detected by LC-MS/MS from PFOS, PFHxS and PFBS are shown in Fig. 9, and consisted of a range of shorter chain PFCA containing from 4 to 8 carbons. When treating the PFSA, the results and trends observed are similar to those shown previously for the PFCA analogues, with the overall yield of shorter chain breakdown products correlating with the chain length of the starting compound, the initial concentration of the PFSA and the overall levels of destruction achieved over time. The quantities of breakdown products detected in the samples similarly accounted for only a small fraction ( $<5\%$ ) of the total fluorine from the destroyed PFSA being converted to shorter chain breakdown products. These findings are consistent with those of Takeuchi et al. who reported that the localised, high temperatures of the plasma interacting with the gas-liquid interface was the primary degradation pathway of PFAS which can directly cleave the carbon-carbon bonds of the molecule and mineralise the perfluoro-carbon radicals into water-soluble hydrogen fluoride and gaseous carbon dioxide and monoxide [48].

As can be seen in Fig. 9 (G, H and I), trace quantities of PFBA at concentrations at or exceeding the 0.01  $\mu\text{g/L}$  detection limit for the instrument were detected forming from the decomposition of PFBS after

40, 60 and 90 min of plasma treatment when treating initial concentrations of 50, 25 and 10  $\mu\text{g/L}$ , respectively, and the concentration ranged between 0.02 and 0.07  $\mu\text{g/L}$  after the full 120 min of plasma treatment. The detection of PFBA as a breakdown product from PFBS during plasma treatment is indicative of a breakdown mechanism involving the attack of electrons or excited argon ions at the carbon-sulfur bond resulting in the cleavage of the sulfonate group from the carbon and a multistep process whereby fluoride is lost from the molecule, and the moiety is replaced with a carboxylic acid group [36].

The breakdown products identified from the plasma treatment of PFOS, PFHxS and PFBS presented across Fig. 9 consisted only of PFCA and the formation of other shorter-chain PFSA could not be observed in any of the samples. The formation of these shorter chains, daughter PFSA from the decomposition of PFOS or PFHxS has been reported in the literature; however, that particular reaction mechanism has been proposed to occur by the reaction between a perfluoroalkyl radical and a sulfonate radical, as opposed to the removal of a perfluorinated carbon in preference to the sulfonate group. [36].

### 3.4. OES spectra discussion

The emission spectra from the argon plasma interacting with the surface of the liquid was recorded and shown in Fig. 10. Most of the peaks were associated with the transition of Ar ( $4p \rightarrow 4s$ ) from 695 to 860 nm, suggesting the presence of high density metastable Ar( $3p^5 4s$ ). As well as electrons and Ar ions, metastable Ar species is known to be highly efficient to enable Penning ionisation and enhance overall chemical reactivity of the system due to its high energy (11.5 eV) and relatively long lifetime.

The large OH(A-X) emission band near 309 nm is due to the fragmentation and excitation of water molecules at the plasma-liquid interface by different plasma species. Apart from the predominant role of high energy electrons, it is worthwhile to note the effective dissociative excitation of water molecules by heavier molecules such as Ar ions or metastable Ar species [68–70]. It is expected that in the interaction with various PFAS molecules, these Ar ions and metastable Ar species may similarly contribute to enhance the dissociation reaction through the charge transfer or dissociative excitation mechanism. [47] In addition, small emission lines consistent with O( $3p \rightarrow 3s$ ) could be observed at the 777 nm and 845 nm, as well as H $\alpha$  emission at 656 nm indicating the transition from 3d to 2p state. The OES supports the presence of various reactive species within the plasma discharge volume which can lead to the various reductive or oxidative reactions mineralising the PFAS molecules as the plasma-liquid interface.

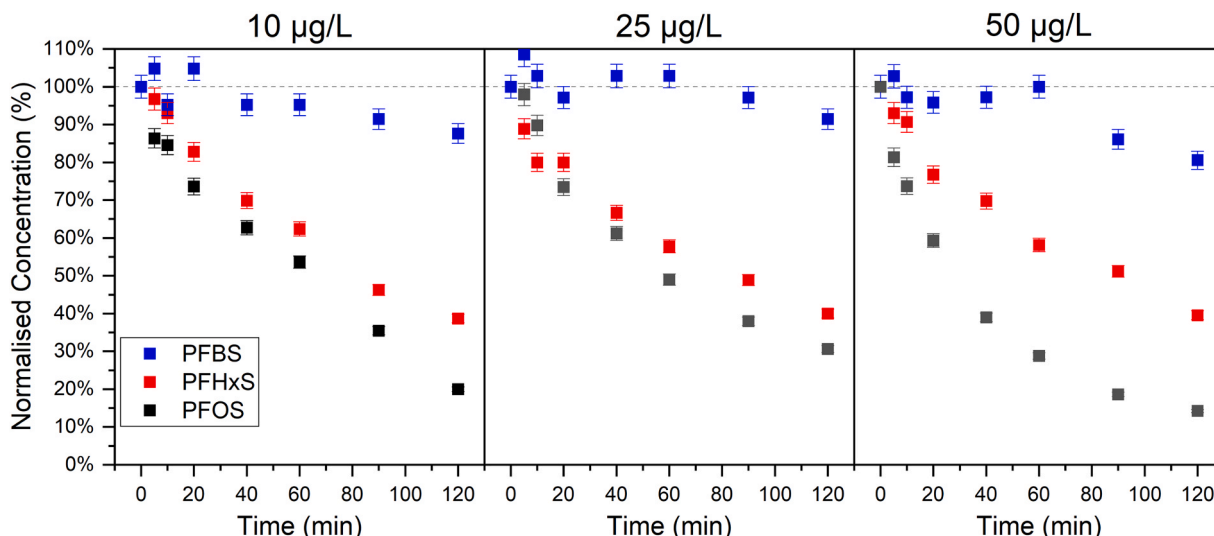
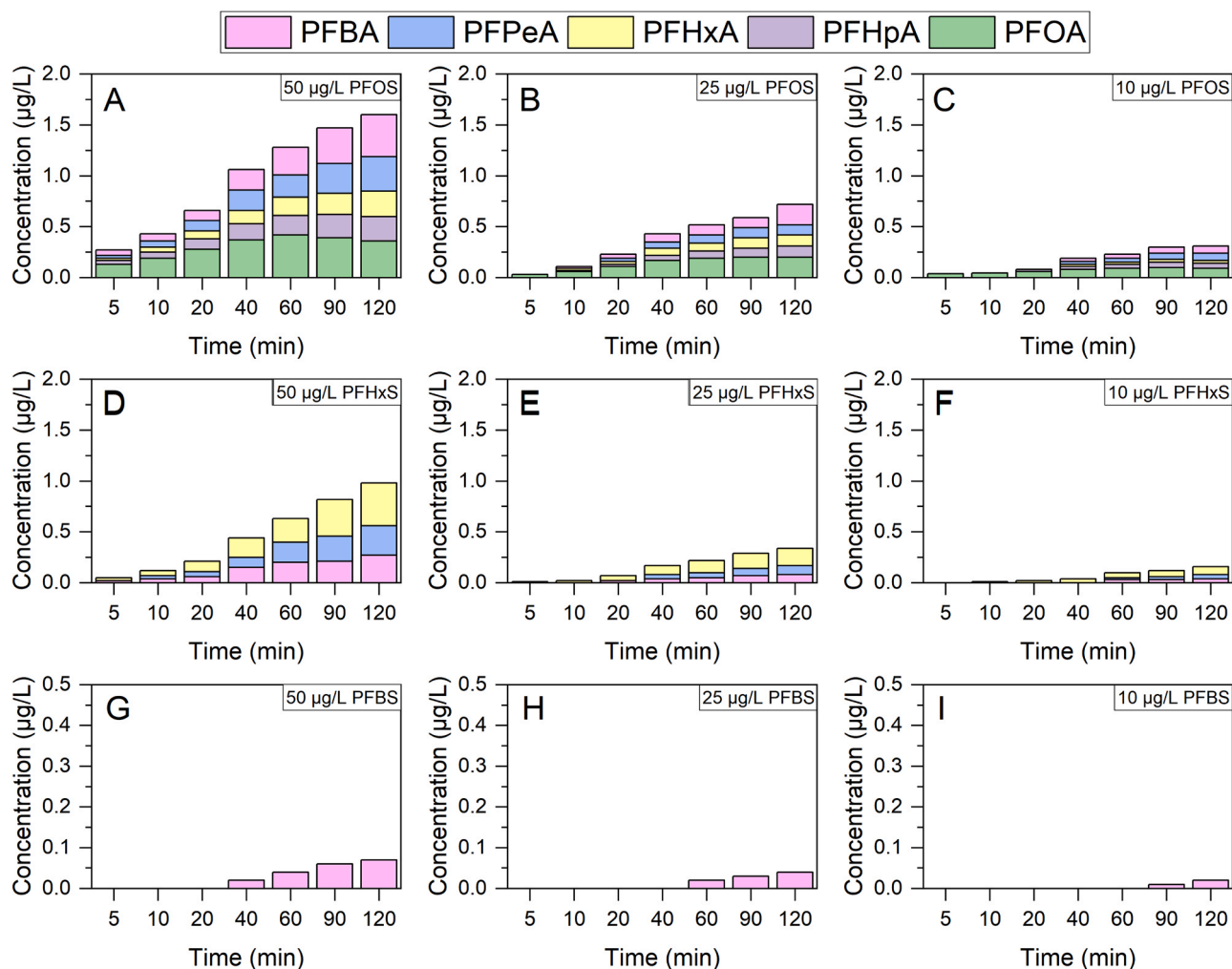
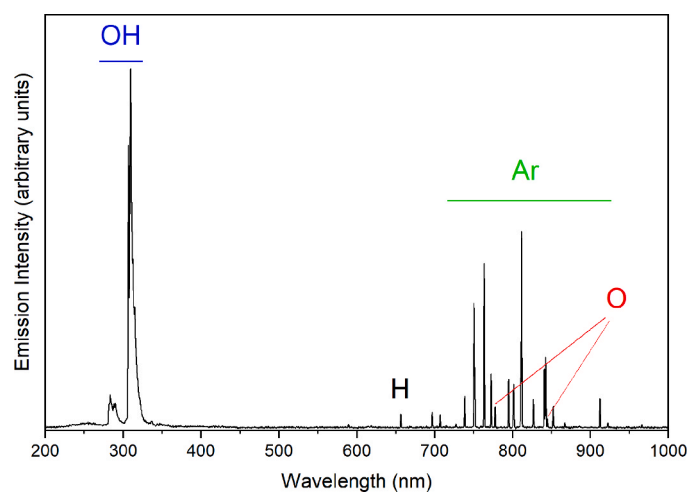


Fig. 8. Normalised concentration of each of the PFSA during plasma treatment at an initial concentration of 10  $\mu\text{g/L}$  (Left), 25  $\mu\text{g/L}$  (Centre) and 50  $\mu\text{g/L}$  (Right).





**Fig. 9.** The concentration of the short-chain PFCAs detected in the liquid samples over time during plasma treatment. PFOS at 50 µg/L (A), 25 µg/L (B), and 10 µg/L (C), PFHxS at 50 µg/L (D), 25 µg/L (E) and 10 µg/L (F), and PFBS at 50 µg/L (G), 25 µg/L (H), and 10 µg/L (I). Note. The concentration range for the Y axis for the PFBS plots (G, H and I) are reduced to 0.5 µg/L to allow for products to be visible.



**Fig. 10.** Optical emission spectrum of the plasma discharge as measured from inside the reactor in the headspace at 200–1000 nm while bubbling argon gas through the water at a flow rate of 1 L/min.

### 3.5. PFAS degradation pathways

The generally accepted breakdown mechanism by which plasma can destroy PFAS directly in water involves the interactions of solvated electrons and argon radical species, as shown in Table 4. Based on mechanisms proposed in the literature and the breakdown products observed in this study, the PFCA likely underwent a several-step, chain-

**Table 4**

Generalised reaction pathways outlining the degradation pathways for PFOS and perfluorocarboxylic acids induced by plasma where n is equal number of carbon atoms of the molecule.

Reaction Pathway	Mechanism	Reference
Chain Shortening Pathway (DHEH Cycle)	$Ar^{\bullet} + C_nF_{2n+1}COO^- \rightarrow Ar + C_nF_{2n+1}COO^{\bullet}$ $C_nF_{2n+1}COO^{\bullet} \rightarrow C_nF_{2n+1} + CO_2$ $C_nF_{2n+1} + H_2O \rightarrow C_nF_{2n+1}OH + H$ $C_nF_{2n+1}OH + H_2O \rightarrow C_{n-1}F_{2n-1}COF + F^- + H^+$ $C_{n-1}F_{2n-1}COF + H_2O \rightarrow C_{n-1}F_{2n-1}COO^- + F^- + 2 H^+$	[71,72]
Ar <sup>+</sup> Bombardment Pathway	$Ar^+ + C_nF_{2n+1}COOH \rightarrow \text{fragment (e.g. } C_xF_y^+)$	[47]
PFOS Degradation	$C_nF_{2n+1}SO_3^- + Ar^{\bullet} \rightarrow C_8F_{17}SO_3^{\bullet} + Ar + e^-$ $C_nF_{2n+1}SO_3^{\bullet} \rightarrow C_nF_{2n+1} + SO_3^-$ $C_nF_{2n+1} + H_2O \rightarrow C_nF_{2n+1}O^- + H^+ + H$ $C_nF_{2n+1}O^- + H_2O \rightarrow C_{n-1}F_{2n-1}COO^- + 2 H^+ + 2 F^-$	[73,74]

shortening reaction pathway involving decarboxylation, hydroxylation, elimination and hydrolysis, known as the DHEH pathway [71]. Following an initial decarboxylation reaction of a PFCA after interaction with argon radicals and/or solvated electrons, an unstable perfluorinated alcohol ( $C_nF_{2n+1}OH$ ) is formed that undergoes hydrogen fluoride (HF) elimination. The resulting acyl fluoride ( $C_{n-1}F_{2n-1}COF$ ) is further hydrolysed by the hydroxyl radicals in the aqueous phase and releases a second fluoride ion, forming a shorter-chain PFCA ( $C_{n-1}F_{2n-1}COO^-$ ).

For the range of PFSA's investigated in this study, the degradation pathways are expected to follow the same stepwise chain shortening DHEH cycle shown in Table 4, with an additional initial reaction step, whereby the sulfonate end group of the PFSA is removed by the bombardment of high energy radicals at the plasma/liquid interface which induces the cleavage of the carbon-sulfur bond. The resulting perfluorocarbon radical is then able to react with water molecules to replace the sulfonate group with a carboxylic acid functional group which displaces fluorine ions from the chain and reduces the length of the molecule by one [73,74].

### 3.6. Overall breakdown kinetics of PFCA and PFSA

The equation below describes the pseudo-first order breakdown kinetics for the range of PFCA and PFSA investigated.

$$\frac{d[PFOX]}{dt} = -k[PFOX]$$

where  $X$  is either a sulfonate (S) or carboxylic acid (A) functional group, and the rate constant  $k$  is a complex function of a number of phenomena, including the surface activity, the available bubble surface area, plasma input power and the surface renewal of the liquid due to agitation induced by the bubbles. The data describing the conversion ( $X$ ) for each compound shown in Fig. 6 and Fig. 8 were used to calculate the rate constants equal to the gradient of the line from the linear regression of  $-\ln(1-X)$  against time at each concentration investigated. The degradation of each compound followed pseudo-first order breakdown kinetics at 10, 25 and 50  $\mu\text{g/L}$  as plotting the logarithm of the concentrations detected at each time point was found to be a linear function with respect to time with a high degree of linearity ( $R^2 = 0.90-0.99$ ). The average rate constants and standard deviations calculated for each PFCA and PFSA over 120 min of plasma treatment are presented in Fig. 11 with the numerical values available in the

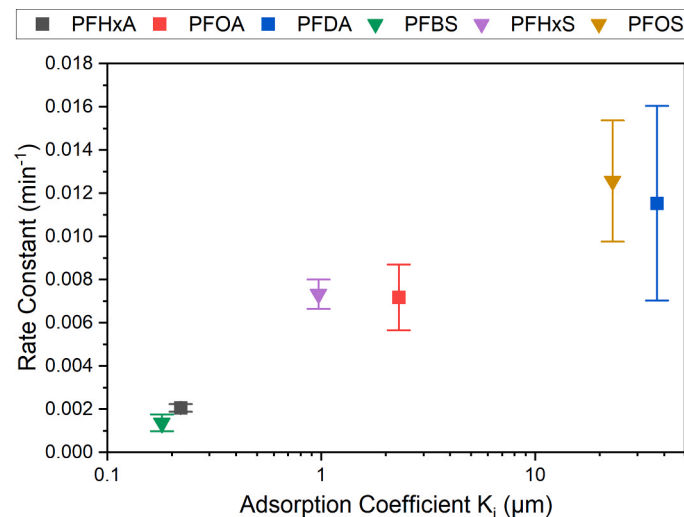


Fig. 11. Average rate constants calculated for each compound over the concentrations investigated (10  $\mu\text{g/L}$ , 25  $\mu\text{g/L}$  and 50  $\mu\text{g/L}$ ) plot against their respective adsorption coefficients with the standard deviation of the results presented as the error bars.

Supplementary Information (Table S2). The rate constants calculated were proportional to the chain length of the compound at each of the concentrations trialled, with the degradation rates calculated demonstrating a linear relationship when comparing the degradation constants calculated for both the PFCAs and PFSA's investigated.

The rate constants for PFOS at each concentration investigated were generally the highest out of all the other PFSA and PFCA compounds investigated, ranging between 1.00 and  $1.55 \times 10^{-3} \text{ min}^{-1}$ . This was true for each rate constant calculated, except for PFDA at an initial concentration of 10  $\mu\text{g/L}$ , which had an exceptionally high rate constant of  $1.67 \pm 0.13 \times 10^{-3} \text{ min}^{-1}$ . The rate constant for PFDA at this concentration was particularly high as it reached an 88% reduction in concentration after 120 min of plasma treatment compared with only 62%, 21% and no conversion for PFOA, PFHxA and PFBA. This particularly high degradation has been proposed to be due to the strong surface activity of this compound, with the adsorption coefficient for PFDA around 60% higher than PFOS at 37  $\mu\text{m}$  compared with 23  $\mu\text{m}$  [75]. This allows PFDA to exert a greater decrease in the surface tension of the solution at lower concentrations compared with other compounds. This compound's strong affinity for the gas-liquid interface can be seen in mixed solutions where PFDA will outcompete other shorter-chain PFCA and accumulate at the gas-liquid interface in greater abundance [76].

When comparing the rate constants for PFOS degradation calculated for the prepared solutions at initial concentrations of 10, 25, and 50  $\mu\text{g/L}$  with those calculated for the degradation of PFOS in the PFAS-contaminated surface water shown previously under the same experimental conditions, the breakdown rates calculated for the prepared, individual solutions were found to be much lower, as shown in Fig. 12. The rate constant calculated for the degradation of PFOS in the contaminated surface water was an order of magnitude larger at  $0.11 \pm 0.01 \text{ min}^{-1}$  compared with the values calculated for the single component solutions, which ranged between 0.01 and  $0.016 \text{ min}^{-1}$ . The overall trends in conversion for PFOS over time were generally linear at each of the concentrations investigated over the 120 min plasma treatment and reached a maximum conversion of 70–85% depending on the initial concentration. In contrast, when plasma treating the contaminated surface water, a much higher breakdown of 99% for PFOS could be reached after only 40 min plasma treatment.

The much higher breakdown rates of PFOS in the contaminated surface water, which contained 14 other PFAS, compared with the degradation of PFOS as an individual component in a 300  $\mu\text{S/cm}$  sodium chloride electrolyte solution is an interesting observation as the rate constants calculated for compounds in mixed PFAS solutions are typically lower than in single component solutions due to competitive adsorption at the gas-liquid interface. [48] Takeuchi et al. reported that the rate constants for PFOA and PFHpA degradation by directly interfacing the plasma within the bubble in a mixed solution at concentrations of 41.4 mg/L and 36.4 mg/L (100  $\mu\text{mol/L}$  of each compound) decreased by 20% compared with the values calculated when treating

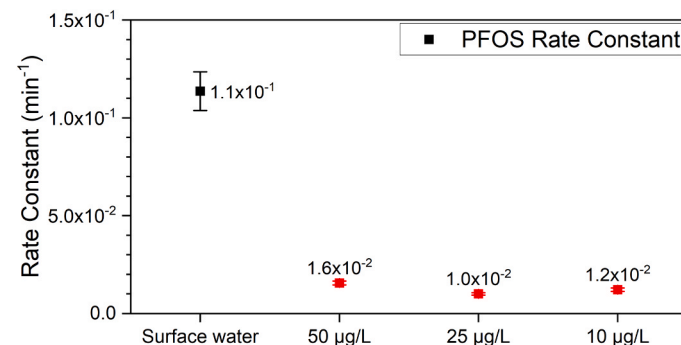


Fig. 12. Rate constants calculated for the breakdown of PFOS in surface water (black) and at each of the concentrations investigated (red) after 120 min of plasma treatment.

the single component solutions at the same concentrations [48]. The other PFAS present in the surface water would have reduced the breakdown rate compared with a single-component solution, and the PFAS composition was determined not to have resulted in such a marked increase in the PFOS breakdown rate.

As the conductivity of the electrolyte solution and the surface water were comparable (300  $\mu\text{S}/\text{cm}$  versus 320  $\mu\text{S}/\text{cm}$ ), the composition of the cations and anions in the surface water was then considered a possible cause of the differing breakdown rates. The surface water contained both monovalent and divalent cations compared with the prepared electrolyte solution, which only contained monovalent sodium ions. Therefore, it was hypothesised that the composition and types of ions in the solution may have increased the overall PFOS degradation rate. The valency of cations is known to affect the surface activity of PFOA, and when comparing the air-water interfacial adsorption coefficients for PFOA in deionised water versus 0.01 M electrolyte solutions of sodium, potassium and calcium chloride, the adsorption coefficients for each respective salt solution increased by 7.4, 6.5 and 74 fold [67]. These results indicate that greater quantities of PFOA can adsorb to the gas-liquid interface when in the presence of divalent cations compared with monovalent cations, which would increase the overall transport of PFOA to the surface to be interfaced with plasma and undergo destruction.

### 3.7. Relationship between cation valency and degradation

The presence of divalent calcium ions on the overall PFAS breakdown rate in the non-thermal plasma bubble column was investigated to experimentally determine if any change in the overall breakdown rate of PFOA could be observed compared with sodium chloride. Divalent cations such as calcium have been used as a metallic activator to enhance the recovery of PFOS and PFOA from dilute aqueous solutions by foam fractionation, with the presence of the divalent calcium having a greater improvement in recovery compared with the monovalent potassium [77]. The presence of an electrolyte, particularly those possessing higher valency, reduces the electrostatic repulsion among the ionic headgroups at the gas-liquid interface of the bubble and increases the activity of the hydrophobic tail in solution which results in an increase in the driving force for adsorption to the bubble from the solution [67,78]. Aqueous solutions of calcium and sodium chloride were prepared to have a conductivity of 300  $\mu\text{S}/\text{cm}$  and were similarly spiked with 50  $\mu\text{g}/\text{L}$  of PFOA and treated in the same reactor and experimental conditions outlined previously. The conductivity of the solutions was kept constant to ensure the behaviour of the plasma discharge remained consistent between experiments. The molar concentrations of the sodium and calcium chloride solutions were determined to be  $\approx 2.4$  mM and  $\approx 1.1$  mM, equivalent to 55 ppm and 44 ppm of sodium and calcium ions present in each respective solution. These concentrations of calcium would be equivalent to 110 mg/L of  $\text{CaCO}_3$ , which would be considered moderately hard water (75–150 mg/L of  $\text{CaCO}_3$ ) by sanitary standards or good quality (60–200 mg/L of  $\text{CaCO}_3$ ) by the Australian Drinking Water Guidelines [79,80]. At these levels, the plasma treated water dosed with calcium will not require any further treatment to remove the calcium.

When comparing the breakdown of PFOA both prepared to an initial conductivity of 300  $\mu\text{S}/\text{cm}$  using either sodium chloride or calcium chloride, the overall reduction in PFOA concentration was  $\approx 10\%$  higher across nearly every time point, as shown in Fig. 13. As the conductivity was kept constant between both experiments, the behaviour of the plasma discharge and overall power consumption was consistent, with the only difference between the experiments being the type of cation in the solution.

The recovery of short-chain PFAS (PFBA, PFPeA, PFHxA and PFHpA) breakdown products and fluoride ions when using calcium chloride approached 99% in the fluorine balance after 120 min of plasma treatment, whereas using sodium chloride as the electrolyte reached 96%, as

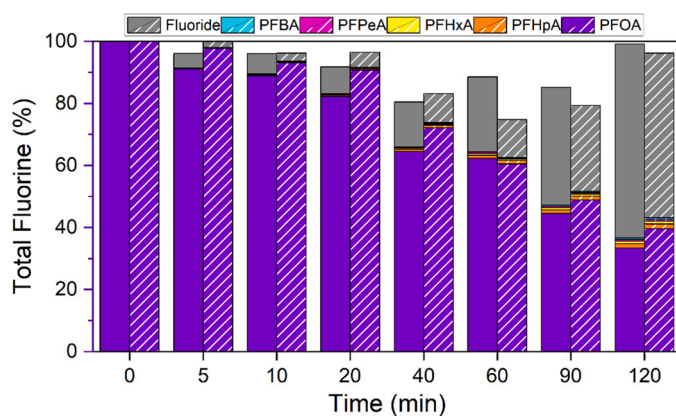


Fig. 13. Overall fluorine balance present in the short-chain PFAS breakdown products and fluoride ions detected at each of the time points during the plasma treatment of a 50  $\mu\text{g}/\text{L}$  PFOA in a 300  $\mu\text{S}/\text{cm}$  solution prepared with either calcium chloride (solid fill) or sodium chloride (dashed).

shown in Fig. 13. The overall yields of shorter chain PFCAs detected for each salt were similar, accounting for 3.4% and 3.6% of the total fluorine in the system after 120 min, while the presence of calcium chloride showed some increase in the overall mineralisation of PFOA, with moderate improvements in the range of 10–20% in the quantities of fluoride ions recovered. The rate constants calculated for the degradation of PFOA over the 120 min of plasma treatment in the 300  $\mu\text{S}/\text{cm}$  electrolyte solution prepared with sodium chloride or calcium chloride were determined to be  $8.1 \times 10^{-3} \text{ min}^{-1}$  and  $8.9 \pm 0.3 \times 10^{-3} \text{ min}^{-1}$ . The modest 10% improvement in PFOA breakdown and greater mineralisation and recovery of fluoride ions was achieved at concentrations of only  $\approx 1\%$  of the electrolyte solutions investigated in Brusseau and Van Glubb (0.01 M), indicating that even low-level quantities of calcium ions (44 ppm) can enhance the treatability of surface active PFAS by plasma treatment [67].

It may be logically proposed that the presence of metallic ions with an oxidation state of  $3^+$ , such as aluminium (III) or iron (III) chloride may further improve the floatation efficiency of PFAS molecules to the surface due to the larger charge [81]. To maintain these metallic ions at this oxidation state in water, the pH must be at relatively strong acidic conditions,  $< 2.4$  for iron (III) or  $< 4$  for aluminium (III); otherwise, the ions will possess a lower charge according to their respective Pourbaix diagrams [82]. Adjusting the pH this low requires the addition of a fairly strong acid, such as hydrochloric or sulfuric acid, which would significantly increase the conductivity of the solution which would influence the behaviour of the plasma discharge and power consumption and hence the experimental conditions would not be comparable with the results here. Additionally, in larger scale applications, the use of either iron or aluminium chloride would incur further operating costs as the treated water would require chemicals to acidify to a pH below either 2.4 or 4 then neutralisation to between 7.0 and 9.0 for discharge into sewerage systems [83].

The presence of calcium ions could have also contributed to the formation of insoluble calcium fluoride ( $\text{CaF}_2$ ) due to the precipitation reaction between calcium and fluoride ions. This technique is commonly used in water treatment applications to remove fluoride ions from waste streams containing high fluoride concentrations in the 10's to 100's of mg/L range [84,85]. Based on the high fluoride and fluorine recoveries in Fig. 13 it is unclear if the precipitation of calcium fluoride occurred, and no cloudiness in the solution or obvious precipitate was observed in any of the samples. However, the precipitation of fluoride as calcium fluoride cannot be entirely dismissed and may have occurred in trace quantities in these experiments. Based on the findings here, calcium chloride has been proposed as a relatively cheap, environmentally benign additive for treatment processes relying on the fractionation



tendencies of PFAS for plasma treatment as used in the treatment reactor used for these experimental studies or in foam floatation applications.

#### 4. Conclusions

Utilising bubbles to transport PFAS to the surface to be interfaced with an argon plasma discharge was found to be effective at achieving degradation of long-chain PFAS (>6 carbons) in prepared solutions and in contaminated surface water. It was shown that PFCAs and PFASs containing  $\geq 6$  carbons were more amenable to degradation using the treatment approach as it exploited their surface activity, with their susceptibility to breakdown correlating with chain length. Concentration strongly influenced the degradation rate, with breakdown rates generally decreasing as concentrations in the solutions reached  $< 5 \mu\text{g/L}$  over time during plasma treatment. Based on the trends of the rate constants calculated for each of the compounds investigated, the rate-limiting factor in the decomposition of these compounds is, therefore the availability of PFAS molecules accumulated at the liquid surface at the liquid-plasma interface.

The rate constants for the degradation of the PFCA and PFSA investigated were calculated at each of the concentrations and demonstrated linear trends in the degradation rate with increasing chain length and exhibited behaviour consistent with a pseudo-first-order kinetic breakdown mechanism. The shortest chain compounds investigated PFBA and PFBS were particularly recalcitrant by this plasma treatment approach due to the low surface activity of these compounds due to the short length of their perfluorinated chain. The concentration of these compounds remained either unchanged after 120 min of plasma treatment at each initial concentration trialled or, in the case of PFBS, marginal reductions of  $\approx 15\%$  could be achieved after 120 min. Losses of these short-chain compounds due to the bubbling action and potential aerosol formation were not observed, nor were there losses observed due to these compounds sticking to the plastic surfaces of the reactor walls. Further investigations are required to improve the treatability of the shorter chain PFAS to address the issue of PFAS contamination in water more adequately.

The fluorine balance approach quantifying the PFCA breakdown products by LC-MS/MS and the inorganic fluoride quantified by IC could account for nearly 100% of the fluorine initially present in the reactor when plasma treating aqueous PFOA solutions. The formation of short-chain by-products from the degradation of the PFCA and PFSA accounted for only  $< 5\%$  of the initial organofluorine present in the parent compound, with the remaining  $\approx 94\%$  of the organofluorine initially present detected as mineralised fluoride ions in the liquid phase after 120 min of plasma treatment.

The presence of calcium ions improved PFOA's breakdown rate and overall mineralisation compared with the same conductivity of  $300 \mu\text{S/cm}$  prepared with sodium chloride as the electrolyte. The concentration of PFOA could be reduced by a further  $\approx 10\%$  after 120 min of plasma treatment when treating the  $300 \mu\text{S/cm}$  calcium chloride solution (66.7%) compared with the sodium chloride solution (60.5%). Calcium chloride may be used as a cheap, environmentally benign additive to improve the floatation efficiency of PFAS to the surface for breakdown by plasma discharge.

#### CRedit authorship contribution statement

**David Alam** Conceptualisation, Equipment Design, Experimental Design, Experiments, Modelling, Writing, **Samiuela Lee** LC-MS method development and analysis, **Jungmi Hong** OES spectra analysis and breakdown pathways, **David F Fletcher** Supervision, Reviewing and Editing **Dale McClure** Conceptualisation, Equipment Design and Experimental Design, Review **David Cook** Review and Analysis, **PJ Cullen** Conceptualisation, Supervision, Reviewing, and **John M Kavanagh** Supervision, Conceptualisation, Equipment Design, Experimental Design, Supervision, Reviewing and Editing.

#### Declaration of Competing Interest

Author P.J. Cullen is the Chief Technology Officer (CTO) of PlasmaLeap Technologies, which supplied the plasma power supply used in this study. Author J.M. Kavanagh has been providing consulting advice to ICD now Ventia on PFAS treatment options and scale up.

#### Data Availability

Data will be made available on request.

#### Acknowledgements

This work was funded by the Australian Research Council's Special Research Initiative on PFAS (SR180200046). Additionally, we acknowledge the support by the Australian Government Research Training Program (RTP) scholarship and David Cook (Ventia, formerly ICD Asia Pacific) for providing the contaminated surface water samples, Dr. Trevor Walker (Ventia, formerly ICD Asia Pacific) for his technical support and Charles Grimison (Ventia) for his time and technical input reviewing this manuscript. This research was facilitated by access to Sydney Mass Spectrometry, a core research facility at the University of Sydney.

#### Appendix A. Supporting information

Supplementary data associated with this article can be found in the online version at [doi:10.1016/j.jece.2023.111588](https://doi.org/10.1016/j.jece.2023.111588).

#### References

- [1] EPA - United States Environmental Protection Agency. PFAS Master List of PFAS Substances. ([https://comptox.epa.gov/dashboard/chemical\\_lists/pfasmaster](https://comptox.epa.gov/dashboard/chemical_lists/pfasmaster)).
- [2] C. Lau, et al., Perfluoroalkyl acids: A review of monitoring and toxicological findings, *Toxicol. Sci.* 99 (2007) 366–394.
- [3] R.C. Buck, et al., Perfluoroalkyl and polyfluoroalkyl substances in the environment: Terminology, classification, and origins, *Integr. Environ. Assess. Manag.* 7 (2011) 513–541.
- [4] E. Kissa, *Fluorinated surfactants and repellents*, Marcel Dekker, 2001.
- [5] J. Glüge, et al., An overview of the uses of per- And polyfluoroalkyl substances (PFAS), *Environ. Sci. Process. Impacts* 22 (2020) 2345–2373.
- [6] H. Viberg, P. Eriksson, Chapter 43 - Perfluorooctane Sulfonate and Perfluorooctanoic Acid, in: R.C.B.T.-R. Gupta, T. D. (Eds.), in *Reproductive and Developmental Toxicology (Second Edition)*, Second E., Academic Press, 2017, pp. 811–827. (<https://doi.org/10.1016/B978-0-12-804239-7.00043-3>).
- [7] R. Renner, Growing Concern Over Perfluorinated Chemicals, *Environ. Sci. Technol.* 35 (2001) 154A–160A.
- [8] J.P. Giesy, K. Kannan, Global distribution of perfluorooctane sulfonate in wildlife, *Environ. Sci. Technol.* 35 (2001) 1339–1342.
- [9] L. Li, H. Zheng, T. Wang, M. Cai, P. Wang, Perfluoroalkyl acids in surface seawater from the North Pacific to the Arctic Ocean: Contamination, distribution and transportation, *Environ. Pollut.* 238 (2018) 168–176.
- [10] G.L. Lescord, et al., Perfluorinated and polyfluorinated compounds in lake food webs from the Canadian High Arctic, *Environ. Sci. Technol.* 49 (2015) 2694–2702.
- [11] M.M. Schultz, D.F. Barofsky, J.A. Field, Quantitative Determination of Fluorotelomer Sulfonates in Groundwater by LC MS/MS, *Environ. Sci. Technol.* 38 (2004) 1828–1835.
- [12] K. Prevedouros, I.T. Cousins, R.C. Buck, S.H. Korzeniowski, Sources, fate and transport of perfluorocarboxylates, *Environ. Sci. Technol.* 40 (2006) 32–44.
- [13] Z. Liu, et al., Risk assessment and source identification of perfluoroalkyl acids in surface and ground water: Spatial distribution around a mega-fluorochemical industrial park, China, *Environ. Int.* 91 (2016) 69–77.
- [14] A.K. Weber, L.B. Barber, D.R. Leblanc, E.M. Sunderland, C.D. Vecitis, Geochemical and Hydrologic Factors Controlling Subsurface Transport of Poly- and Perfluoroalkyl Substances, Cape Cod, Massachusetts, *Environ. Sci. Technol.* 51 (2017) 4269–4279.
- [15] J.R. Lang, B.M.K. Allred, G.F. Peaslee, J.A. Field, M.A. Barlaz, Release of Per- and Polyfluoroalkyl Substances (PFASs) from Carpet and Clothing in Model Anaerobic Landfill Reactors, *Environ. Sci. Technol.* 50 (2016) 5024–5032.
- [16] K. Hoffman, et al., Perfluorooctanoic Acid Exposure and Cancer Outcomes in a Contaminated Community: A Geographic Analysis, *Environ. Health Perspect.* 121 (2013) 318–323.
- [17] C8 Science Panel. C8 Probable Link Reports. (<http://www.c8sciencepanel.org/prob-link.html>) (2012).
- [18] K. Steenland, L. Zhao, A. Winquist, C. Parks, Ulcerative colitis and perfluorooctanoic acid (PFOA) in a highly exposed population of community

- residents and workers in the Mid-Ohio Valley, *Environ. Health Perspect.* 121 (2013) 900–905.
- [19] S. Woodard, J. Berry, B. Newman, Ion exchange resin for PFAS removal and pilot test comparison to GAC, *Remediation* 27 (2017) 19–27.
- [20] F. Dixit, B. Barbeau, S.G. Mostafavi, M. Mohseni, PFOA and PFOS removal by ion exchange for water reuse and drinking applications: Role of organic matter characteristics, *Environ. Sci. Technol.* 5 (2019) 1782–1795.
- [21] C.Y. Tang, Q.S. Fu, A.P. Robertson, C.S. Criddle, J.O. Leckie, Use of reverse osmosis membranes to remove perfluorooctane sulfonate (PFOS) from semiconductor wastewater, *Environ. Sci. Technol.* 40 (2006) 7343–7349.
- [22] J. Thompson, et al., Removal of PFOS, PFOA and other perfluoroalkyl acids at water reclamation plants in South East Queensland Australia, *Chemosphere* 82 (2011) 9–17.
- [23] C. Boo, et al., High Performance Nanofiltration Membrane for Effective Removal of Perfluoroalkyl Substances at High Water Recovery, *Environ. Sci. Technol.* 52 (2018) 7279–7288.
- [24] P. McCleef, et al., Removal efficiency of multiple poly- and perfluoroalkyl substances (PFASs) in drinking water using granular activated carbon (GAC) and anion exchange (AE) column tests, *Water Res* 120 (2017) 77–87.
- [25] X. Xiao, B.A. Ulrich, B. Chen, C.P. Higgins, Sorption of Poly- and Perfluoroalkyl Substances (PFASs) Relevant to Aqueous Film-Forming Foam (AFFF)-Impacted Groundwater by Biochars and Activated Carbon, *Environ. Sci. Technol.* 51 (2017) 6342–6351.
- [26] M. Inyang, E.R.V. Dickenson, The use of carbon adsorbents for the removal of perfluoroalkyl acids from potable reuse systems, *Chemosphere* 184 (2017) 168–175.
- [27] V.A. Arias Espana, M. Mallavarapu, R. Naidu, Treatment technologies for aqueous perfluorooctanesulfonate (PFOS) and perfluorooctanoate (PFOA): A critical review with an emphasis on field testing, *Environ. Technol. Innov.* 4 (2015) 168–181.
- [28] R. James Wood, et al., Ultrasonic degradation of perfluorooctane sulfonic acid (PFOS) correlated with sonochemical and sonoluminescence characterisation, *Ultrason. Sonochem.* 68 (2020), 105196.
- [29] B. Wu, et al., Rapid Destruction and Defluorination of Perfluorooctanesulfonate by Alkaline Hydrothermal Reaction, *Environ. Sci. Technol. Lett.* 6 (2019) 630–636.
- [30] Hao, S. et al. Hydrothermal Alkaline Treatment for Destruction of Per- and Poly fluoroalkyl Substances in Aqueous Film-Forming Foam. (2021) doi:(10.1021/acs.est.0c06906).
- [31] H. Komiyama, H. Inoue, 20 Absorption of nitrogen oxides into water, *Chem. Eng. Sci.* 35 (1980) 154–161.
- [32] Q. Zhuo, et al., Degradation of perfluorinated compounds on a boron-doped diamond electrode, *Electrochim. Acta* 77 (2012) 17–22.
- [33] M. Trojanowicz, A. Bojanowska-Czajka, I. Bartosiewicz, K. Kulisa, Advanced Oxidation/Reduction Processes treatment for aqueous perfluorooctanoate (PFOA) and perfluorooctanesulfonate (PFOS) – A review of recent advances, *Chem. Eng. J.* 336 (2018) 170–199.
- [34] A.L. Garcia-Costa, A. Savall, J.A. Zazo, J.A. Casas, K. Groenen Serrano, On the Role of the Cathode for the Electro-Oxidation of Perfluorooctanoic Acid, *Catalysts* 10 (2020) 902.
- [35] A. Mahyar, et al., Development and Application of Different Non-thermal Plasma Reactors for the Removal of Perfluorosurfactants in Water: A Comparative Study, *Plasma Chem. Plasma Process* 39 (2019) 531–544.
- [36] R.K. Singh, et al., Breakdown products from perfluorinated alkyl substances (PFAS) degradation in a plasma-based water treatment process, *Environ. Sci. Technol.* 53 (2019), acs.est.8b07031.
- [37] R.P. Joshi, S.M. Thagard, Streamer-Like Electrical Discharges in Water: Part II. Environmental Applications, *Plasma Chem. Plasma Process* 33 (2013) 17–49.
- [38] B.R. Locke, M. Sato, P. Sunka, M.R. Hoffmann, J.S. Chang, Electrohydraulic discharge and nonthermal plasma for water treatment, *Ind. Eng. Chem. Res.* 45 (2006) 882–905.
- [39] L. Huang, W. Dong, H. Hou, Investigation of the reactivity of hydrated electron toward perfluorinated carboxylates by laser flash photolysis, *Chem. Phys. Lett.* 436 (2007) 124–128.
- [40] X. Liu, et al., Photochemical decomposition of perfluorochemicals in contaminated water, *Water Res* 186 (2020).
- [41] C.E. Schaefer, C. Andaya, A. Urtiaga, E.R. McKenzie, C.P. Higgins, Electrochemical treatment of perfluorooctanoic acid (PFOA) and perfluorooctane sulfonic acid (PFOS) in groundwater impacted by aqueous film forming foams (AFFFs), *J. Hazard. Mater.* 295 (2015) 170–175.
- [42] C.E. Schaefer, et al., Electrochemical treatment of perfluorooctanoic acid and perfluorooctane sulfonate: Insights into mechanisms and application to groundwater treatment, *Chem. Eng. J.* 317 (2017) 424–432.
- [43] A.J. Lewis, et al., Rapid degradation of PFAS in aqueous solutions by reverse vortex flow gliding arc plasma, *Environ. Sci. Water Res. Technol.* (2020), <https://doi.org/10.1039/c9ew01050e>.
- [44] R.K. Singh, et al., Rapid Removal of Poly- and Perfluorinated Compounds from Investigation-Derived Waste (IDW) in a Pilot-Scale Plasma Reactor, *Environ. Sci. Technol.* (2019), <https://doi.org/10.1021/acs.est.9b02964>.
- [45] C. Nau-Hix, T.M. Holsen, & Mededovic Thagard, S. Optimization of a gas-liquid plasma reactor for water treatment applications: Design guidelines and electrical circuit considerations, *Plasma Process. Polym.* 19 (2022) 2200036.
- [46] E. Psillakis, M.R. Hoffmann, A.J. Colussi, J. Cheng, Enrichment Factors of Perfluoroalkyl Anionic Surfactants at the Air / water, *Interface* 11 (2009) 11179.
- [47] J.P. Wiens, T.M. Miller, S.G. Ard, A.A. Viggiano, N.S. Shuman, Elementary Reactions Leading to Perfluoroalkyl Substance Degradation in an Ar+/-e-Plasma, *J. Phys. Chem. A* 126 (2022) 9076–9086.
- [48] N. Takeuchi, et al., Plasma-liquid interfacial reaction in decomposition of perfluoro surfactants, *J. Phys. D. Appl. Phys.* 47 (2014).
- [49] A. Fridman, A. Chirokov, A. Gutsol, Non-thermal atmospheric pressure discharges, *J. Phys. D. Appl. Phys.* 38 (2005).
- [50] A.L. George, G.F. White, Optimization of the methylene blue assay for anionic surfactants added to estuarine and marine water, *Environ. Toxicol. Chem.* 18 (1999) 2232–2236.
- [51] M. Söregård, V. Franke, R. Tröger, L. Ahrens, Losses of poly- and perfluoroalkyl substances to syringe filter materials, *J. Chromatogr. A* 1609 (2020).
- [52] D.W. Connell, The Octanol-Water Partition Coefficient, *Handb. Ecotoxicol.* (1997) 775–784, <https://doi.org/10.1002/9781444313512.ch35>.
- [53] D.J. Burns, P. Stevenson, P.J.C. Murphy, PFAS removal from groundwaters using Surface-Active Foam Fractionation, *Remediation* 31 (2021) 19–33.
- [54] T. Buckley, et al., Using foam fractionation to estimate PFAS air-water interface adsorption behaviour at ng/L and µg/L concentrations, *Water Res* 239 (2023), 120028.
- [55] US EPA. Estimation Programs Interface Suite™ for Microsoft® Windows, v 4.11. (2020).
- [56] A. Lampic, J.M. Parnis, Property Estimation of Per- and Polyfluoroalkyl Substances: A Comparative Assessment of Estimation Methods, *Environ. Toxicol. Chem.* 39 (2020) 775–786.
- [57] M.L. Brusseau, The influence of molecular structure on the adsorption of PFAS to fluid-fluid interfaces: Using QSPR to predict interfacial adsorption coefficients, *Water Res* 152 (2019) 148–158.
- [58] J.A. Field, J. Seow, Properties, occurrence, and fate of fluorotelomer sulfonates, *Crit. Rev. Environ. Sci. Technol.* 47 (2017) 643–691.
- [59] P.H.N. Vo, et al., Foam fractionation of per- and polyfluoroalkyl substances (PFASs) in landfill leachate using different cosurfactants, *Chemosphere* 310 (2023), 136869.
- [60] R.K. Singh, E. Brown, S. Mededovic Thagard, T.M. Holsen, Treatment of PFAS-containing, Land. leachate Using Enhanc. Contact Plasma React. *J. Hazard. Mater.* 408 (2020), 124452.
- [61] R.K. Singh, et al., Removal of Poly- And Per-Fluorinated Compounds from Ion Exchange Regenerant Still Bottom Samples in a Plasma Reactor, *Environ. Sci. Technol.* (2020), <https://doi.org/10.1021/acs.est.0c02158>.
- [62] D. Lu, S. Sha, J. Luo, Z. Huang, X. Zhang Jackie, Treatment train approaches for the remediation of per- and polyfluoroalkyl substances (PFAS): A critical review, *J. Hazard. Mater.* vol. 386 (2020).
- [63] Y.L. Liu, M. Sun, Ion exchange removal and resin regeneration to treat per- and polyfluoroalkyl ether acids and other emerging PFAS in drinking water, *Water Res* 207 (2021), 117781.
- [64] A. Maimaiti, et al., Competitive adsorption of perfluoroalkyl substances on anion exchange resins in simulated AFFF-impacted groundwater, *Chem. Eng. J.* 348 (2018) 494–502.
- [65] G.R. Stratton, et al., Plasma-Based Water Treatment: Efficient Transformation of Perfluoroalkyl Substances in Prepared Solutions and Contaminated Groundwater, *Environ. Sci. Technol.* 51 (2017) 1643–1648.
- [66] N. Takeuchi, et al., Discharge conditions for efficient and rapid decomposition of perfluorooctane sulfonic acid (PFOS) in water using plasma. *Int. J. Plasma, Environ. Sci. Technol.* 14 (2020) 1–12.
- [67] M.L. Brusseau, & Van Glubt, S. The influence of surfactant and solution composition on PFAS adsorption at fluid-fluid interfaces, *Water Res* 161 (2019) 17–26.
- [68] P.J. Bruggeman, N. Sadeghi, D.C. Schram, V. Linss, Gas temperature determination from rotational lines in non-equilibrium plasmas: A review, *Plasma Sources Sci. Technol.* 23 (2014).
- [69] P. Bruggeman, D.C. Schram, O.H. On, production in water containing atmospheric pressure plasmas, *Plasma Sources Sci. Technol.* 19 (2010).
- [70] S. Novicki, J. Krenos, Absolute quenching cross section for collisions between Ar (3P<sub>0,2</sub>) and H<sub>2</sub>O, *J. Chem. Phys.* 89 (1988) 7031–7033.
- [71] Etching. in *Principles of Plasma Discharges and Materials Processing* 571–617 (John Wiley & Sons, Ltd, 2005). doi:<https://doi.org/10.1002/0471724254.ch15>.
- [72] R. Hayashi, H. Obo, N. Takeuchi, K. Yasuoka, Decomposition of Perfluorinated Compounds in Water by DC Plasma within Oxygen Bubbles, *Electr. Eng. Jpn. (Engl. Transl. Denki Gakkai Ronbunshi)* 190 (2015) 9–16.
- [73] K. Yasuoka, K. Sasaki, R. Hayashi, An energy-efficient process for decomposing perfluorooctanoic and perfluorooctane sulfonic acids using dc plasmas generated within gas bubbles, *Plasma Sources Sci. Technol.* 20 (2011), 034009.
- [74] M.J. Bentel, et al., Defluorination of Per- and Polyfluoroalkyl Substances (PFASs) with Hydrated Electrons: Structural Dependence and Implications to PFAS Remediation and Management, *Environ. Sci. Technol.* (2019), acs.est.8b06648, <https://doi.org/10.1021/acs.est.8b06648>.
- [75] M.L. Brusseau, S. Van Glubt, The influence of molecular structure on PFAS adsorption at air-water interfaces in electrolyte solutions, *Chemosphere* 281 (2021), 130829.
- [76] J.A.K. Silva, W.A. Martin, J.E. McCray, Air-water interfacial adsorption coefficients for PFAS when present as a multi-component mixture, *J. Contam. Hydrol.* 236 (2021), 103731.
- [77] M. Mulder, *Basic Principles of Membrane Technology. Separation and Purification Technology*, vol. 173, Springer Netherlands, 1996.
- [78] K. Shinoda, M. Hato, T. Hayashi, Physicochemical properties of aqueous solutions of fluorinated surfactants, *J. Phys. Chem.* 76 (1972) 909–914.
- [79] C.N. Sawyer, P.L. McCarty, Chemistry for sanitary engineers, McGraw-Hill, 1967.
- [80] National Health and Medical Research Council. *Australian drinking water guidelines Paper 6: National Water Quality Management Strategy, version 3.4 Updated October 2017*. (2011).



- [81] Y.C. Lee, P.Y. Wang, S.L. Lo, C.P. Huang, Recovery of perfluorooctane sulfonate (PFOS) and perfluorooctanoate (PFOA) from dilute water solution by foam flotation, *Sep. Purif. Technol.* 173 (2017) 280–285.
- [82] P. Pedferri, in: P. Pedferri (Ed.), *Pourbaix Diagrams BT - Corrosion Science and Engineering*, Springer International Publishing, 2018, pp. 57–72, [https://doi.org/10.1007/978-3-319-97625-9\\_4](https://doi.org/10.1007/978-3-319-97625-9_4).
- [83] NSW Department of Planning Industry and Environment. *Liquid Trade Waste Management Guidelines 2021*. ([https://www.industry.nsw.gov.au/\\_data/assets/pdf\\_file/0010/147088/trade-waste-management-guidelines.pdf](https://www.industry.nsw.gov.au/_data/assets/pdf_file/0010/147088/trade-waste-management-guidelines.pdf)) (2021).
- [84] G. El Diwani, S.K. Amin, N.K. Attia, S.I. Hawash, Fluoride pollutants removal from industrial wastewater, *Bull. Natl. Res. Cent.* 46 (2022).
- [85] M. Markovic, S. Takagi, L.C. Chow, S. Frukhtbeyn, Calcium fluoride precipitation and deposition from 12 mmol/L fluoride solutions with different calcium addition rates, *J. Res. Natl. Inst. Stand. Technol.* 114 (2009) 293–301.